Cytometry
PART A
Journal of the International Society for Advancement of Cytometry

Quantitative Comparison of Polar Approach Versus Fitting Method in Time Domain FLIM Image Analysis

A. Leray,[1] C. Spriet,[1] D. Trinel,[1] R. Blossey,[2] Y. Usson,[3] L. Héliot[1]*

[1]Interdisciplinary Research Institute, Science and Technology University of Lille, USR 3078 CNRS, Biophotonique Cellulaire Fonctionnelle, Parc de la Haute Borne, 59650 Villeneuve d'Ascq, France

[2]Interdisciplinary Research Institute, Science and Technology University of Lille, USR 3078 CNRS, Biological Nanosystems, Parc de la Haute Borne, 59650 Villeneuve d'Ascq, France

[3]Laboratoire TIMC-IMAG, Université Joseph Fourier, UMR 5525 CNRS, RFMQ, Domaine de la Merci, 38710 La Tronche, France

Received 27 August 2010; Revision Received 30 September 2010; Accepted 21 October 2010

Additional Supporting Information may be found in the online version of this article.

Grant sponsors: CNRS (GdR2588 and MRCT), Région Nord Pas de Calais, European Regional Developmental Funds, Leica Microsystems partnership, Agence Nationale de la Recherche; Grant number: ANR 07-PFTV-01101.

*Correspondence to: Dr. Laurent Héliot, Interdisciplinary Research Institute, CNRS USR 3078, Parc de la Haute Borne, 50 Avenue Halley, 59650 Villeneuve d'Ascq, France

Email: laurent.heliot@iri.univ-lille1.fr

Published online 2 December 2010 in Wiley Online Library (wileyonlinelibrary.com)

DOI: 10.1002/cyto.a.20996

ISAC
International Society for Advancement of Cytometry

Abstract

We calculate here analytically the performance of the polar approach (or phasor) in terms of signal-to-noise ratio and *F* values when performing time-domain Fluorescence Lifetime Imaging Microscopy (FLIM) to determine the minimal number of photons necessary for FLIM measurements (which is directly related to the *F* value), and compare them to those obtained from a well-known fitting strategy using the Least Square Method (LSM). The importance of the fluorescence background on the lifetime measurement precision is also investigated. We demonstrate here that the LSM does not provide the best estimator of the lifetime parameter for fluorophores exhibiting mono-exponential intensity decays as soon as fluorescence background is superior to 5%. The polar approach enables indeed to determine more precisely the lifetime values for a limited range corresponding to usually encountered fluorescence lifetime values. These theoretical results are corroborated with Monte Carlo simulations. We finally demonstrate experimentally that the polar approach allows distinguishing in living cells two fluorophores undetectable with usual time-domain LSM fitting software. © 2010 International Society for Advancement of Cytometry

Key terms

fluorescence lifetime imaging microscopy (FLIM); living cell; molecular interactions; phasor; *F*-value; LSM

Fluorescence Lifetime Imaging Microscopy (FLIM), which relies on the measurement of the fluorescence lifetime at each pixel in an image, is now routinely performed in many biological and biophysical laboratories. Since this fluorescence lifetime is sensitive to the local environment of the fluorophore [e.g. [Ca^{2+}], pH, temperature, viscosity, energy transfer (1)], a large number of biologically relevant questions can now be assessed without the need for ratiometric measurements. For example, it becomes possible to visualize and to quantify the dynamic interactions between proteins in vivo by detecting lifetime modifications associated with Förster Resonance Energy Transfer (FRET) occurring between two fluorescent probes (a donor and an acceptor) (2,3).

Up to now, a large number of different techniques have been developed and have been used to measure the fluorescence lifetime. These techniques can be divided into two main groups: frequency domain methods (4–6) and time domain methods (7–9). In this article, we limit our study to this second group.

In time domain methods, a series of short pulses of light excites a fluorescent sample and the consecutive intensity $I(t)$ emitted by this sample is measured. The intensity profile, which can be a single or multi-exponential decay, varies according to:

$$I(t) = \sum_i a_i \exp\left(-\frac{t}{\tau_i}\right) \quad (1)$$

In most cases, the determination of the different lifetimes τ_i and contributions a_i are achieved by fitting the collected data at each pixel with this equation with two or more unknowns. The major problems with this fitting method are that it requires

computation time and a high level of expertise to obtain reliable results, due to the large number of existing minimization algorithms, the large number of unknown parameters, the correlation between lifetimes and species contributions and the low number of detected photons in biological samples.

To simplify the analysis of FLIM images and to make it accessible to the non-expert user, alternative strategies have been developed (10–12). Among all these techniques, the polar plot or phasor initially described by Jameson et al. (13) and then developed by different groups (14,15) is a promising approach. In the time domain, it consists of converting the standard temporal FLIM image into frequency domain data by calculating the Fourier sine and cosine transforms for each experimental fluorescence decay. These values are then represented in a two-dimensional histogram which corresponds to the polar image. With this nonfitting approach, a fast and visual representation of fluorescence lifetimes is obtained which greatly facilitated the analysis of FLIM data. Compared to the standard well-known fitting method, the qualitative interest of this original approach is obvious and it has been widely reported in the literature (12,14,15). However, to the best of our knowledge, none of these numerous studies addresses the quantitative issues of sensitivity, minimum lifetime resolution or Signal-to-Noise Ratio (SNR).

In this article, we describe and perform a quantitative and complete comparison of the two distinct strategies: the fitting method and the polar analysis. For quantifying the performance of each approach, we employ the F value introduced by Gerritsen et al. (16) which is defined as $F = (\sigma_\tau/\tau)/(\sigma_N/N)$ where σ_τ is the standard deviation in repeated measurements of the lifetime value τ and σ_N is the standard deviation of the number of detected photons N. In fluorescence microscopy, this number of collected photons N is Poisson distributed, which implies that the SNR is $N/\sigma_N = 1/\sqrt{N}$. The F value becomes then $F = \sqrt{N} \times \sigma_\tau/\tau$.

Ultimately, with an ideal lifetime determination procedure, the number of detected photons required to measure both fluorescence lifetime and intensity is identical. In this case, the SNR of the lifetime measurement σ_τ/τ corresponds exactly to the SNR in fluorescence microscopy and the F value is equal to unity. However, in real FLIM experiments, σ_τ/τ is always superior to $1/\sqrt{N}$ and the F value is then always greater than unity. Consequently, the more F is close to unity, the better is the lifetime determination procedure.

In the first part of this manuscript, we present the theoretical F values for an idealized fluorophore exhibiting monoexponential intensity decay and theoretically study the impact of the fluorescence background on these values. We then confront these theoretical values to computed ones obtained from Monte Carlo simulations. We finally corroborate these simulations with experimental results acquired in the temporal domain with the time correlated single photon counting (TCSPC) technique.

Theoretical Consideration

We begin by considering an idealized fluorescent sample whose intensity decay is a monoexponential of lifetime τ. In temporal domain methods, the fluorescence emitted by this sample is caused by the excitation with a Dirac light pulse at time $t = 0$. This signal is then recorded by an idealized background-free lifetime acquisition system composed of k time channels of width T/k [the Instrumental Response Function (IRF) of this acquisition system is then identical to the excitation Dirac pulse]. In this case, the fluorescence intensity function $f(t)$ is

$$f(t) = \frac{\exp(-t/\tau)}{\tau\left(1 - \exp\left(-\frac{T}{\tau}\right)\right)}, \quad 0 \le t \le T \tag{2}$$

which is normalized so that its integral value over the finite width T of the measurement window equals unity.

To correctly estimate the unique unknown parameter τ from a given dataset, several statistical methods exist (17,18). In this work, we focus our attention on the estimation procedure that gives the highest accuracy with the minimal number of data. From the exhaustive work performed by Hall and Sellinger (18), it has been demonstrated that the most precise strategy to determine the lifetime parameter is by fitting the collected data with either the Least Square Method (LSM) or the Maximum Likelihood Estimator (MLE). This fitting method has been commonly used and it has been adapted in most iteration-based commercial software. The variance of the lifetime determined with the fitting method is also provided in Refs. 18 and 19. From these calculations, we can deduce the F value as

$$F_{\text{fit}} = \frac{k}{r}\sqrt{1-\exp(-r)} \times \left(\frac{\exp(r/k)[1-\exp(-r)]}{\left(\exp\left(\frac{r}{k}\right)-1\right)^2} - \frac{k^2}{\exp(r)-1}\right)^{-1/2} \tag{3}$$

where $r = T/\tau$. For an infinitely small temporal interval of measurement (or, in other words, for an infinite number of time channels k), we can simplify this equation as

$$F_{\text{fit}} \to \sqrt{\frac{2 - 2\cosh(r)}{2 + r^2 - 2\cosh(r)}}, \quad k \to \infty \tag{4}$$

This expression corresponds to the minimal F value accessible with an ideal fluorescence lifetime acquisition system. For example, to measure a lifetime $\tau = 2.5$ ns with an acquisition temporal window of $T = 12.5$ ns, this limit is equal to $F_{\text{fit}} = 1.0981$ and it is almost reached for $k = 64$ time channels ($F_{\text{fit}} = 1.0985$).

If we consider now that there is a constant background noted b underlying the intensity decay, the fluorescence intensity function $f(t)$ is then defined as

$$f(t) = \frac{b}{T} + (1-b) \times \frac{\exp(-t/\tau)}{\tau\left(1 - \exp\left(-\frac{T}{\tau}\right)\right)}, \quad 0 \le t \le T \tag{5}$$

In this case, there is no analytical expression for the F value of the fitting method.

Of course, it can be calculated numerically according to Ref. 19. For instance, for the previously described example with an added constant background $b = 0.1$, we obtain $F_{\text{fit}} = 1.3596$. As

anticipated, when a background is added to the measurement data, the precision of the lifetime determination deteriorates and hence the F value is increased. Complete plots of F value of the fitting method as a function of the parameter r with or without an added background are illustrated in black in Figure 1.

To avoid these complex fitting algorithm strategies, a promising alternative approach has been developed and recently employed in the time domain. This is the polar analysis also called phasor. Technically, this new representation is obtained by calculating the Fourier sine and cosine transforms (also noted $[u; v]$ coordinates) of all temporal decays $f(t)$. With this mathematical operation, each point in the polar representation corresponds to a single intensity decay curve present in each FLIM image pixel. More details can be found in (12,20). The u- and v- coordinates of a monoexponential temporal decay $f(t)$ are then simply defined by

$$u(\omega) = \frac{\int_0^T f(t) \times \cos(\omega t) dt}{\int_0^T f(t) dt} = \frac{1}{1 + \omega^2 \tau^2} \quad (6)$$

$$v(\omega) = \frac{\int_0^T f(t) \times \sin(\omega t) dt}{\int_0^T f(t) dt} = \frac{\omega \tau}{1 + \omega^2 \tau^2} \quad (7)$$

where ω is the laser repetition frequency. From these equations, we can deduce the phase and modulation lifetime values τ_m and τ_φ which are well known parameters in the frequency domain (1)

$$\tau_m = \frac{1}{\omega} \left(\frac{1}{u(\omega)^2 + v(\omega)^2} - 1 \right)^{1/2} \quad (8)$$

$$\tau_\varphi = \frac{1}{\omega} \left(\frac{v(\omega)}{u(\omega)} \right) \quad (9)$$

To determine the theoretical F value of the polar approach, we have applied for the temporal domain the method described by Philip and Carlsson in frequency domain lifetime imaging techniques (21). In this work, we consider a fluorescent sample exhibiting monoexponential intensity decay. For such a sample, the phase and modulation lifetimes are equivalent. We then define the mean lifetime $\tau = (\tau_m + \tau_\varphi)/2$ and calculate analytically the F value in this case (the detailed calculation is presented in the Supporting Information Appendix). We obtain

$$F_{\text{polar}} = \frac{1}{2} \left(1 + \frac{4\pi^2}{r^2} \right) \times \sqrt{\frac{8\pi^2 + 5r^2}{16\pi^2 + r^2}} \quad (10)$$

with the same parameter $r = T/\tau$. Note that this theoretical F value has been obtained with a continuous probability distribution (which corresponds to an infinite number of time channels k). It is then obvious that in this case, F is independent of k. Moreover, the numerical integration errors of the u and v coordinates that may occur in real experiments are not considered in these calculations.

By applying this equation to the same fluorescent sample of lifetime $\tau = 2.5$ ns acquired on a temporal window of $T = 12.5$ ns, we found $F_{\text{polar}} = 1.3617$. The theoretical accuracy of the fluorescence lifetime measurement performed with the polar approach is then slightly worse (25%) than one obtained with the standard fitting method.

When a background intensity b is added to the idealized fluorescence intensity $f(t)$, we can also calculate analytically the expression of F value deduced from the polar procedure (see Supporting Information Appendix for details). This expression is

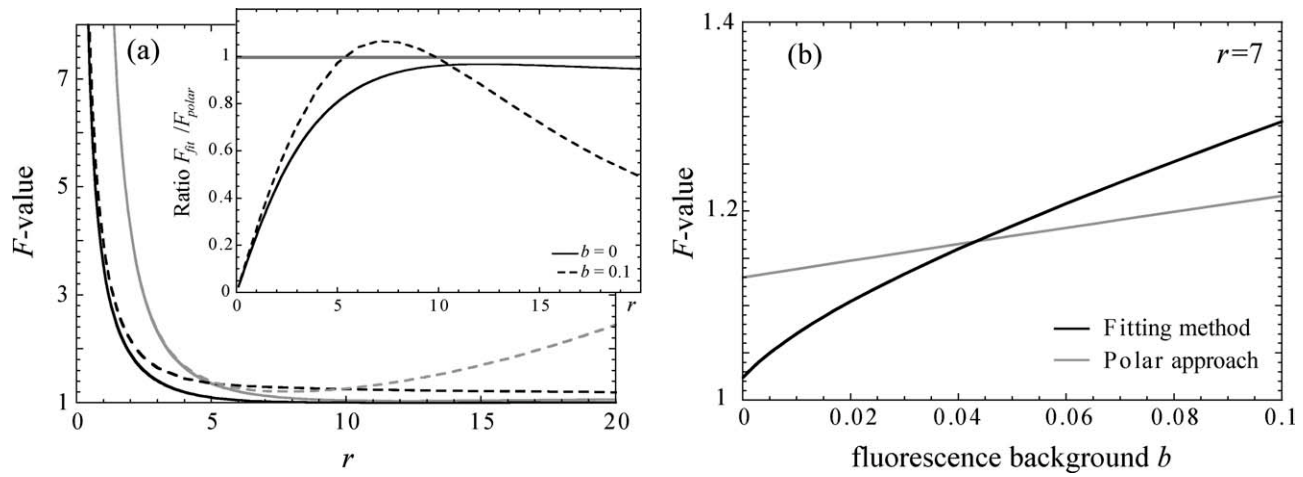

Figure 1. (**a**) Plots of theoretical F value of both the fitting method (in black) and the polar approach (in gray) as a function of $r = T/\tau$ where T is the total width of the measurement window and τ is the fluorescence lifetime. Calculations are performed for mono-exponential temporal decay with (dashed lines) and without fluorescence background b (plain lines). The theoretical ratio $F_{\text{fit}}/F_{\text{polar}}$ is represented in the inset. Note that the ratio of 1 is also indicated as a gray line. (**b**) Theoretical F values of both the fitting method (in black) and the polar approach (in gray) as a function of the fluorescence background b for $r = 7$. The polar approach becomes more precise than the fitting method when the fluorescence background is superior to 5%.

$$F_{\text{polar}} = \frac{1}{2}\left(1+\frac{4\pi^2}{r^2}\right)\sqrt{\frac{1}{16\pi^2+r^2}\left(8\pi^2+5r^2+b\frac{r^2(-16\pi^4+56\pi^2r^2+3r^4)}{32\pi^4}\right)} \quad (11)$$

Note that we well retrieve Eq. (10) in the absence of fluorescence background ($b = 0$). If we consider the same previous example with an added background $b = 10\%$, we have $F_{\text{polar}} = 1.3991$ which is almost identical to F_{fit} obtained with the fitting method. It is thus interesting to plot F_{polar} as a function of r (cf. Fig. 1) and to compare F_{polar} and F_{fit}. We remark in Figure 1 that in the presence of background, the theoretical gain of the polar analysis over the fitting procedure is improved in comparison with the background free case for $r < 10$ (or $\tau > 1.25$ ns when $T = 12.5$ ns and $b = 0.1$). The lifetime precision accessible with the polar approach can even be better than that obtained with the well-known fitting method (or in other words $F_{\text{fit}}/F_{\text{polar}}>1$) for the lifetime range $1.25 < \tau < 2.5$ ns (with $T = 12.5$ ns) when the fluorescence background b is superior to 5% (Fig. 1b).

However, in all these calculations, in order to resolve F values analytically, we have considered a constant known background which is not true in typical experimental conditions. In a usual acquisition situation, this parameter is totally unknown and it also has to be estimated. As previously shown by Köllner and Wolfrum for the fitting method (19), F_{fit} becomes notably larger than the expected value when b is unknown and it can even be doubled. Concerning the polar approach, the effects of an unknown background on the lifetime measurement have never been studied. In the following sections of this manuscript, we study these effects by considering simulated data and we then confront the results to the theory.

Materials and Methods

Monte Carlo Simulations

To assess the effect of fluorescence background on the calculated lifetimes, Monte Carlo simulations are performed on a computer by generating FLIM images with controlled parameters. Succinctly, each simulated temporal decay (composed of N photons divided in k time channels) is computed from a random number generator whose density probability function is the theoretical fluorescence profile $I(t)$ described in Eq. (1). These simulated N photons are Poisson distributed to mimic the characteristics of the optical acquisition system. A more detailed description of the Monte Carlo algorithm used is provided in (10). To simulate the fluorescence background we finally added to each temporal decay, a number N_b of photons which are also independently Poisson distributed with mean value N_b and standard deviation $\sqrt{N_b}$ corresponding to the photon shot noise. To be as close as possible to usual experimental conditions, we assume a laser repetition frequency of 80 MHz (which corresponds to a pulse repetition period of 12.5 ns) and a measurement window width $T = 11.25$ ns. All simulations are performed with 64 time channels since the F value limit is almost reached for this number of intervals.

FLIM Image Analysis

To compare both analysis methods (polar approach and fitting strategy), the simulated data are afterward processed without fixing any parameters (all parameters free).

With the polar approach, fluorescence lifetimes are calculated with a custom-made software named MAPI (IRI, USR 3078 CNRS, BCF). This software computes the polar image by calculating the Fourier sine and cosine transforms of all experimental points and calculates the phase and modulation lifetimes τ_m and τ_φ defined in Eqs. (8) and (9) and then the mean lifetime $\tau = (\tau_m + \tau_\varphi)/2$. For a sample with a single exponential intensity decay, this mean lifetime corresponds to the desired lifetime value. To obtain correct lifetime values, we need that temporal decays are background corrected (see Supporting Information Appendix for details). To do this, we estimate an average background that we subtract from the experimental FLIM images. This average background is calculated by summing the three first temporal channels in all image pixels and then by dividing this sum by three times the total number of pixels.

When the commonly-used fitting strategy is applied, the lifetime values are determined by fitting each simulated point with mono-exponential intensity decay using the standard least square method with Levenberg-Marquardt algorithm (7). To do this, the commercially available SPC Image software (version 2.9.9.29107, Becker & Hickl GmbH) is used. We employ the multiexponential decay fitting model (with a single component) with trapezoid integration, minimal parameter constraints (min lifetime: 20ps; max lifetime: 30,000 ps; min ratio: 1) and standard algorithmic settings (10 iterations and $\Delta\chi^2 = 0.001$). We first apply this fitting strategy to the subtracted FLIM image described previously, but the minimization algorithm in this case is not stable which leads to a shift in the mean fluorescence lifetime and a degradation of standard deviation (data not shown). In this work, we perform our fitting strategy on the whole FLIM image.

Cell Culture and Transfection

HEK293 cells stably expressing histone H2A fused to Cyan Fluorescent Protein (CFP) were grown in plastic flasks at 37°C in 5% CO_2 in Dulbecco's modified Eagle's medium (GIBCO/BRL) supplemented with 10% fetal calf serum. Cells were plated on 32-mm diameter glass coverslips 18 h before transfection. FuGENE HD (Roche Diagnostics) was used according to the manufacturer's recommendations for transfection of memb-eGFP (memb-eGFP plasmid was derived from memb-mCherry (22) and was kindly provided by Dr. Franck Riquet). This protein labels cell membranes. For FLIM imaging, culture medium was replaced by L15 medium (GIBCO/BRL) that allows pH stabilization during experiments. The transfected cells were placed in a temperature-controlled chamber during FLIM acquisitions.

Results

Monte Carlo Simulations

To evaluate and to compare the precision of both FLIM image analysis procedures (fitting methods and polar approach), we have represented in the first part of this work the simulated F values as a function of $r = T/\tau$ for each analysis strategy and we have compared them with the theory. We then have computed FLIM images of 64 × 64 pixels with a single fluorescence lifetime varying from 0.5 to 10 ns. For each image, we have considered two different background levels: $b = 0$ and $b = 0.1$. From these simulated data, we have deduced the mean lifetime and the standard deviation of the lifetime determination for both analysis procedures and hence derived the corresponding F value. The results obtained are reported in Figure 2.

In the absence of background, the lifetime precision of each FLIM image analysis strategy is almost identical (which is materialized by F values of the same order in Fig. 2). With the polar approach, we note that our simulated results are in good accordance with the theory which is not the case for the fitting method. This can be explained by the fact that the theoretical F value is independent of the minimization algorithm considered. In fact, there exist a large number of different minimization algorithms that have specific advantages like robustness, precision, or short calculation times and that may notably influence the F values (in this work we have employed the commonly used Levenberg-Marquardt algorithm). When adding a fluorescence background ($b = 0.1$), the simulated F values determined from the standard fitting method are now extremely different from the theory (Fig. 2). We note also that the simulated F values calculated with the polar approach (in accord with the theory) are significantly lower than those obtained with the standard fitting procedure for $3.5 < r < 17.5$ (which almost corresponds to $0.5 < \tau < 3$ ns). In other words, theoretically and experimentally, for fluorescence lifetime values commonly encountered in biology and when additional background is present, the measurement accuracy accessible with the polar approach is better than those obtained with the fitting method.

To illustrate the importance of this result, we have then studied the smallest resolvable lifetime difference for both analysis methods. To do this, we have computed FLIM images containing four adjacent regions with usual lifetimes of 2.4, 2.5, 2.6, and 2.7 ns, respectively (Fig. 3). If the number of background photons is zero ($b = 0$), each image region is clearly discernible and one clearly sees a separation between individual peaks in the histograms, whatever analysis method applied. In the absence of background, the precision of the measurement allows to resolve lifetime differences between individual regions (100 ps). When background is added to the data in the same manner as previously described (to obtain $b = 0.1$), each individual peak corresponding to each lifetime region is clearly separated with the polar approach whereas it is not the case with the fitting method, probably due to the convergence of the minimization algorithm to a local, rather than a global minimum. Note that, as anticipated from Figure 2, the measurement precision increases when the fluorescence lifetime decreases.

Additional simulations have been performed to quantify the lifetime resolution in FLIM images. These simulated data are constituted of two distinct regions of 8,192 pixels. One of them has been computed with a single fluorescence lifetime $\tau = 2.5$ ns and the other one with a single smaller variable lifetime. For quantifying the minimal lifetime resolution we then plot the lifetime distribution for each simulated image and we use the notion of contrast C defined as

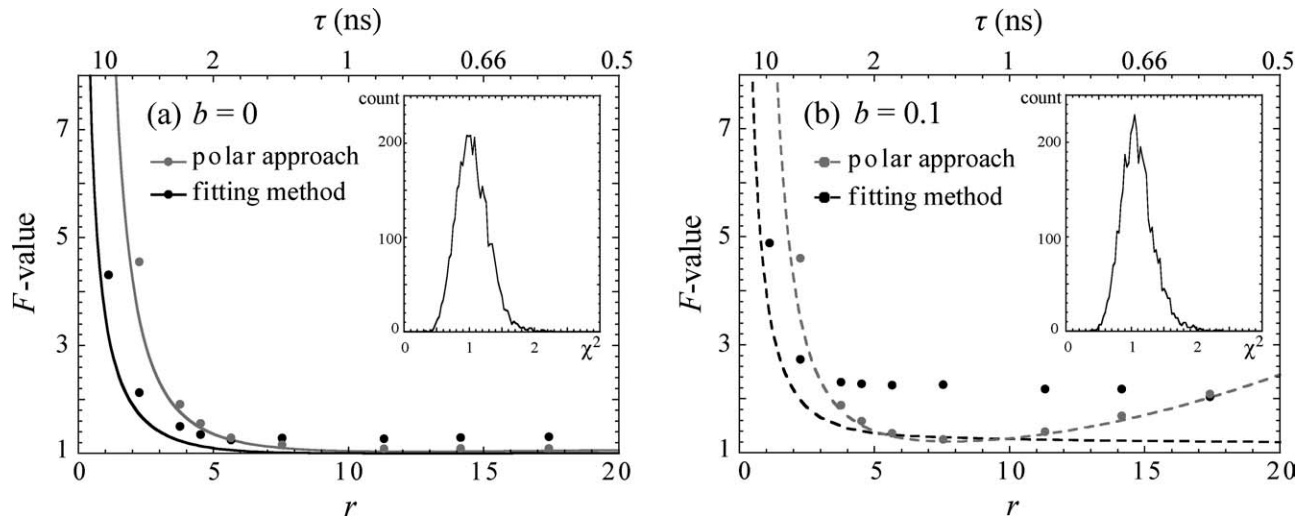

Figure 2. Plots of F-value as a function of $r = T/\tau$ without (**a**) or with (**b**) fluorescence background. The lifetime values τ calculated with a measurement window $T = 10$ ns are also indicated in the upper part of the plots. The theoretical F values (lines) are compared to the simulated results (dots) for both the standard fitting method (in black) and the polar approach (in gray). All simulations are performed with 4,096 pixels and $N = 900$ photons. We have also represented in the insets the histograms of the fitting estimator χ^2 for $r = 5.66$, to show that the minimization algorithm is well converging and stable.

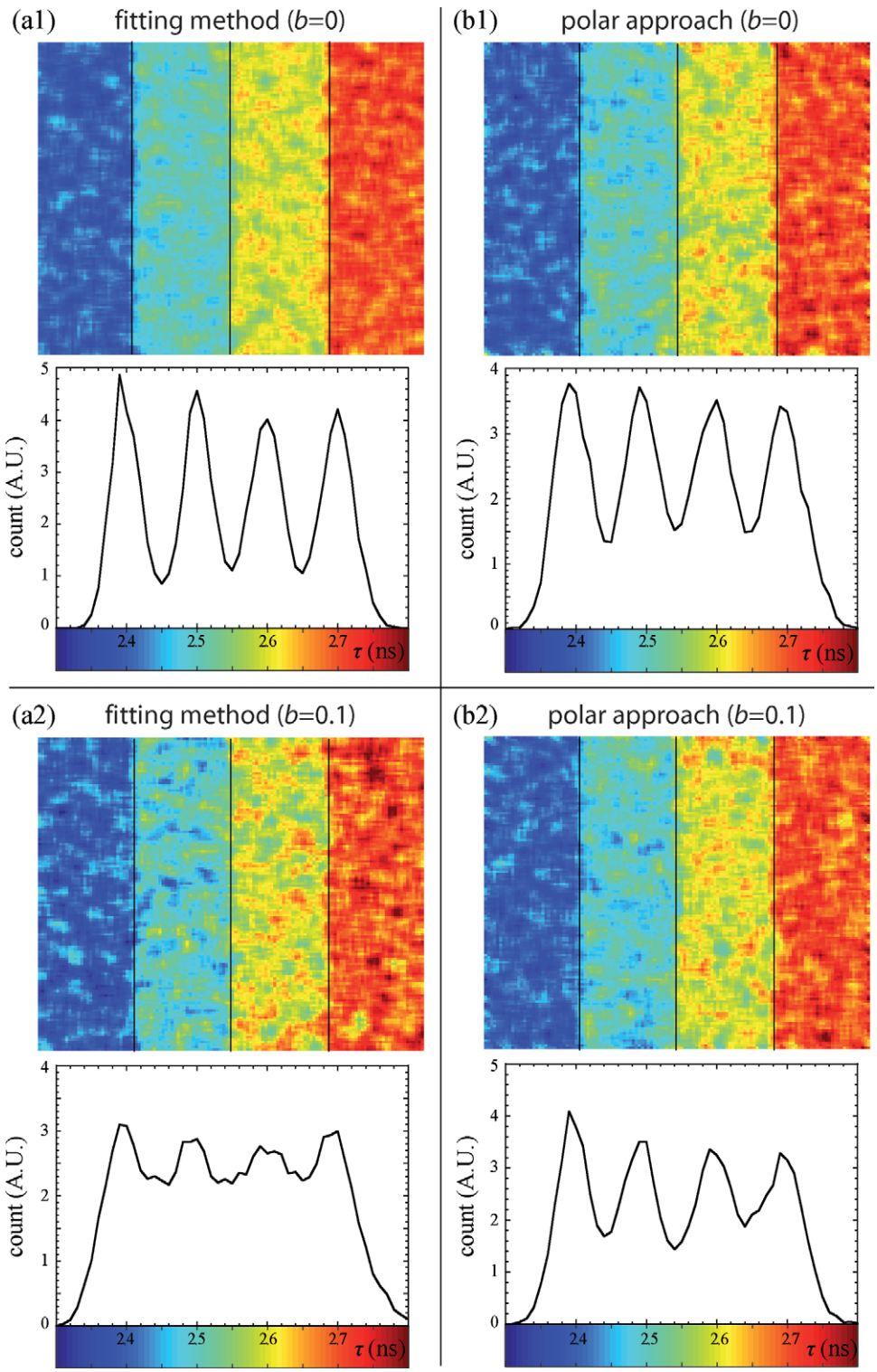

Figure 3. Simulated images to establish the smallest resolvable lifetime differences of both the fitting method (**a**) and the polar approach (**b**). All images are composed of four adjacent regions of 4,096 pixels, each with increasing lifetimes varying from 2.4 to 2.7 ns, with 100 ps steps. Two fluorescence background levels are considered: $b = 0$ (1) and $b = 0.1$ (2). Below each image, the lifetime distributions of the entire image of $N = 16{,}384$ pixels is plotted. To improve the signal-to-noise ratio, the intensity images are binned with a factor $n = 2$ corresponding to a surface of 5×5 pixels. [Color figure can be viewed in the online issue, which is available at wileyonlinelibrary.com.]

$$C = \frac{I_{max} - I_{min}}{I_{max} + I_{min}} \quad (12)$$

where I_{max} is the mean maximum count of both peaks of the lifetime distribution and I_{min} is the minimum count found between them. Using this definition, several resolution criteria can be used. For example, the Rayleigh criterion, which is well known in spatial resolution, corresponds to a contrast $C = 26.4\%$. In this work, we have considered that the separation between the two peaks is achieved for a contrast superior to 50%. Figure 4 shows this minimal lifetime resolution as a function of SNR for two different Signal-to-Background Ratio (SBR) (SBR $= N/N_b$): an infinite SBR (or $N_b = 0$) and SBR $= 10$. Note that the SNR ratio is only dependent on the number of simulated photons N and it is equal to $N/\sqrt{N}$. It is then completely different from SBR $= N/N_b$, which is associated with both N and N_b (the number of background photons).

For each SBR, the smallest resolvable lifetime exhibits a nonlinear dependence on the *SNR* (cf. Fig. 4). When simulations are fluorescence background free, the minimum lifetime differences detectable in FLIM images with the standard fitting method are slightly better than those calculated with the polar approach (as anticipated from Fig. 2). For $N_b = 0.1N$, the situation is notably different. We note indeed a non-negligible degradation of the lifetime resolution when FLIM images are analyzed with the standard fitting method whereas they are almost unaffected by the background with the polar approach. As previously mentioned, with additional background as an unknown parameter, the robustness of the minimization algorithm used in the fitting method is altered (convergence to local minimum). Consequently, the smallest lifetime differences resolvable by analyzing FLIM images with the standard fitting method are clearly inferior to that reachable with the polar approach. In other words, FLIM image analysis with the polar approach enables to separate two fluorescence lifetimes which are not distinguishable with the standard fitting method. Moreover, this gain in lifetime resolution with the polar approach is nonlinearly dependent on the SNR and it is particularly significant when SNR < 100, or $N < 10{,}000$ photons (cf. Fig. 4b). For example, a SNR of 20 and 60 results respectively in a gain in minimum resolvable lifetime difference of 310 and 50 ps. We would like to insist on the fact that these SNR values (SNR $= 20$ and 60) which are equivalent to a total number of photons of 400 and 3,600, respectively considering Poisson shot noise, correspond to typical experimental conditions encountered during FLIM acquisitions. Note that this measurement precision between two regions within the same image, which can be described as intra-image resolution, is completely different from the measurement precision between two different images (or inter-image precision). This inter-image precision is also an important issue to correctly quantify the performance of each FLIM image analysis procedure. In this work, we have not considered the inter-image precision directly but we have focused on a related quantity: the sensitivity which is defined as the minimal number of photons necessary to achieve a given accuracy in lifetime measurements. This fundamental quantity is hence required for minimizing the FLIM acquisition time and consequently reducing potential photodamage in sensitive samples such as living cells and tissues.

To evaluate this sensitivity, we have simulated FLIM images with different numbers of photons N and have then compared the measured fluorescence lifetimes deduced by both the fitting method and the polar approach with the true simulated lifetimes. When at least 99% of the 4,096 image pixels have the desired lifetime precision, we have considered that the lifetime measurement was correctly performed. The results are presented in Figure 5 for a simulated single lifetime $\tau =$ 2.5 ns with two different SBR.

In the absence of background photons ($N_b = 0$), as anticipated, the minimal number of collected photons N

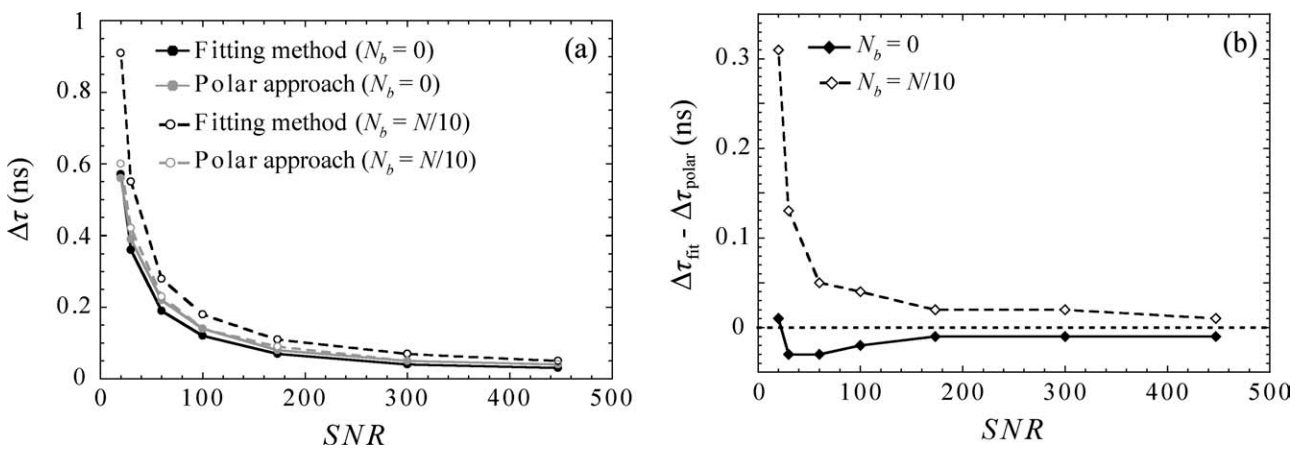

Figure 4. (**a**) Minimum resolvable lifetime differences between two regions within single lifetime image ($\Delta\tau$) detectable with the fitting method (black) and the polar approach (gray) in the absence ($N_b = 0$) and presence of background ($N_b = N/10$) as a function of signal-to-noise ratio SNR. To emphasize the superiority of the polar approach over the standard fitting method we represent the inter-image resolution difference $\Delta\tau_{fit} - \Delta\tau_{polar}$ in (**b**). Results are shown for $\tau = 2.5$ ns, $T = 11.25$ ns and a lifetime contrast superior to 50%. Note that the zero difference is also indicated as a black dotted line.

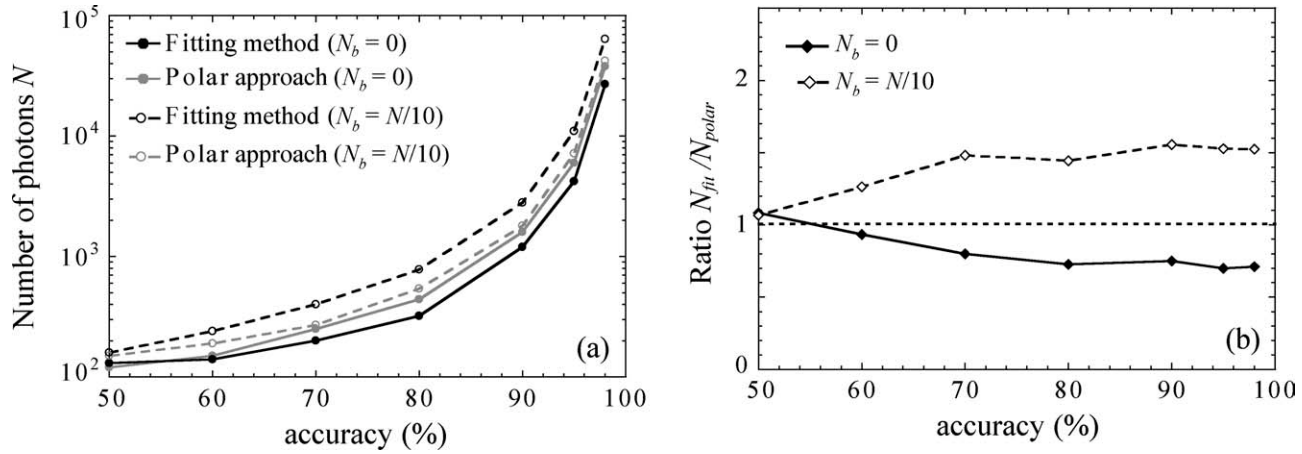

Figure 5. (**a**) Comparison of the sensitivity reachable with both the standard fitting method (in black) and the polar approach (in gray) for SBR = ∞ and SBR = 10. Simulated lifetime measurements are performed for a fluorophore with a single lifetime component τ = 2.5 ns and T = 11.25 ns (r = 4.5). (**b**) Ratio of the previous sensitivity curves of the fitting method over the polar approach without (N_b = 0) or with fluorescence background N_b = N/10) to stress the interest of the polar approach. When this ratio is equal to unity (represented in black dotted line), both methods are equivalent. The gain in sensitivity with the polar approach is materialized by a ratio superior to 1.

increases when the desired precision is higher and the sensitivity of FLIM image analysis performed with the fitting method is slightly improved in comparison with those performed with the polar approach. For example, 38,000 and 27,000 photons are required for measuring a lifetime τ = 2.5 ns with a precision of 99% by applying respectively the polar approach and the fitting method. In other words, the ratio of the minimal number of photons required in the fitting method over those required in the polar approach $N_{\text{fit}}/N_{\text{polar}}$ is slightly inferior to unity (cf. Fig. 5b). When fluorescence background is present (SBR = 10), the sensitivity of the polar approach which is almost identical to the background free case becomes significantly higher than the sensitivity of the standard fitting method. As shown in Figure 5b, the minimal number of photons required for reaching an accuracy superior to 70% is reduced by a factor of 3/2 when using the polar approach. For instance, if we consider the previously described example, one need 42,000 and 64,000 photons to measure with 99% accuracy a lifetime of τ = 2.5 ns with respectively the polar plot and the fitting method for b = 0.1. Therefore, with the polar analysis, we can achieve similar precision lifetime measurements with shorter acquisition time in comparison with commonly-used fitting procedures.

Experimental Application

To corroborate the previous simulated results and to confirm the interest of the polar analysis over standard fitting procedures, we realized FLIM acquisition on living cells. For these FLIM experiments, a modelocked Ti:sapphire laser beam is focused into a sample, and the resulting two photon excitation fluorescence (TPEF) is epicollected and routed to an MCP-PMT detector (R3809U-52, Hamamatsu). This system detailed in Ref. 9 allows accurate and reproducible acquisition of fluorescence lifetimes. HEK293 transfected cells were imaged with a 63× oil-immersion objective (NA = 1.4, Leica), scanned with 400-Hz frequency and the resulting images were stored in a 128 × 128 pixel frame. The femtosecond Ti:Sa oscillator was tuned to the wavelength of 880 nm and the laser power was limited to about 3 mW (at objective focal point) to avoid photobleaching. The overall acquisition time of a complete image took 5 min. For each experiment, we verified that fluorophores had not been photodamaged and/or photobleached.

When performing FLIM image analysis of HEK293 cells co-expressing H2A-CFP and memb-eGFP (Fig. 6), we clearly distinguish with the polar procedure two spots corresponding to two different fluorescent labels. One spot localized on the semi-circle is attributed to eGFP which is a well-known single exponential decay fluorophore (Fig. 6a). The other one located inside the semi-circle indicates that multiple lifetime components are present; it is allocated to the CFP label. Given that these two spots are well discriminated with their phase values, we represent the phase lifetime τ_ϕ image in Figure 6c. As anticipated with the polar plot, this FLIM image exhibits two lifetime populations: the higher lifetime values are confined in the membrane (eGFP) and the lower values in the nuclei (CFP). From this FLIM image, each fluorescent label is thus easily identified.

If we compare this image with the image obtained with the standard fitting procedure (Fig. 6d), one can clearly evaluate the advantage of the polar analysis over the standard fitting method. As indicated by lifetime histograms in Figure 6b, the polar approach allows separating two fluorescent lifetime populations (labeling respectively the cell membrane and the nucleus) which are not distinguishable with the standard fitting procedure.

Discussion

We have demonstrated herein that the widely used standard fitting method is extremely dependent on the fluorescence

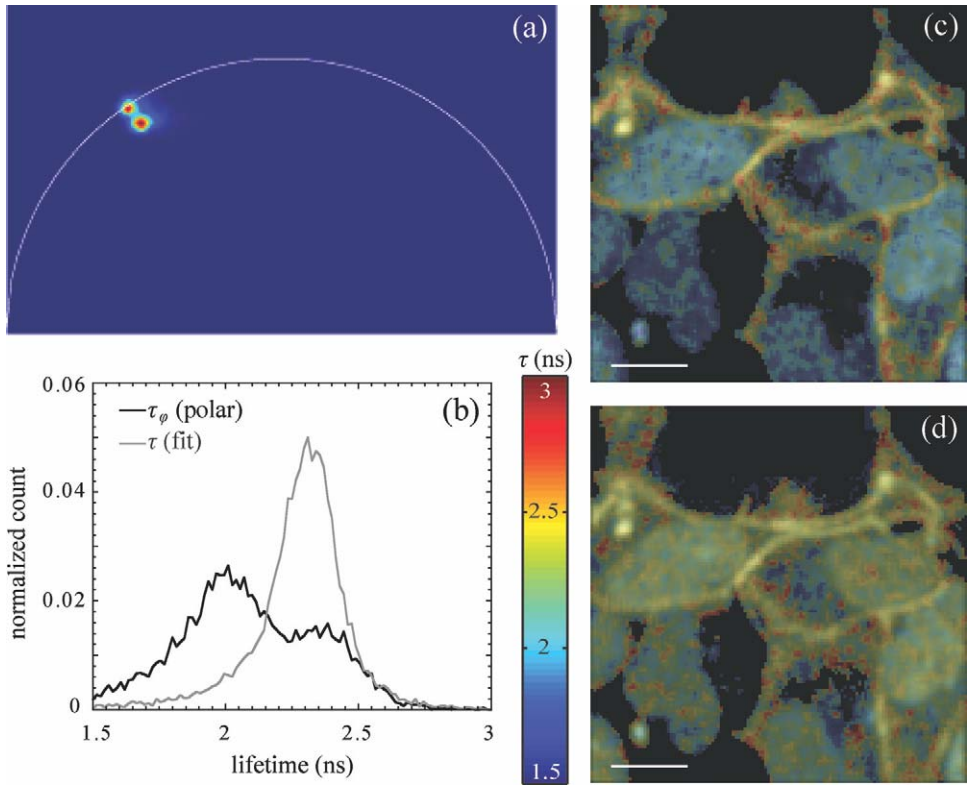

Figure 6. (**a**) Polar representation of HEK293 cells co-expressing H2A-CFP and memb-eGFP. Note that both fluorescent labels are well separated. The fluorescence lifetime images obtained with the polar approach and the standard fitting procedure are represented respectively in (**c**) and (**d**). Scale bar: 50 μm. The corresponding lifetime histograms of both methods are plotted in (**b**). [Color figure can be viewed in the online issue, which is available at wileyonlinelibrary.com.]

background which is always present in time-domain FLIM image experiments. The signal-to-noise ratio as well as the sensitivity and the lifetime resolution are severely degraded when this parasite background has to be estimated (19) due to the fitting algorithm strategy. The situation is notably different when FLIM image analysis is performed with the polar approach. We have thus demonstrated that the signal-to-noise ratio as well as the sensitivity and lifetime resolution calculated with the polar approach are weakly affected by this fluorescence background. The benefit of using this nonfitting polar approach becomes then evident in biological samples.

As previously mentioned, the simulated F values achieved with the fitting method and presented in this work are significantly higher than anticipated by theory. This is largely due to the fact that the robustness of the minimization algorithm used in the fitting method is altered when the fluorescence background is an additional unknown fitting parameter (the minimization algorithm has probably found a local minimum). To improve the concordance between simulation and theory and to converge towards the global, rather than a local minimum, a simple solution would consist in using more robust fitting algorithms. However this will extend the fluorescence lifetime determination time. We have performed all our lifetime measurements by using widely used and commercially available fitting software called SPCImage (Becker & Hickl) using the Levenberg-Marquardt algorithm which has the advantage to be a good compromise between optimization speed and lifetime precision. We have also tested another FLIM image analysis software called Tri2 (23) from the Gray Cancer Institute for Radiation Oncology and Biology (University of Oxford, UK) and obtained comparable results when fitting pixel by pixel with Levenberg-Marquardt algorithm and all parameters free (data not shown). It would be interesting in a future work to compare these results with other fitting algorithms and estimation procedures (like the maximum likelihood estimation). To the best of our knowledge, such an exhaustive study has never been reported in the presence of fluorescence background.

Even if we use a fitting algorithm enabling to perfectly match simulated and theoretical F values (ideal case), we remind the reader that the polar approach allows reaching higher lifetime precision than the fitting method in presence of low background ($b > 0.05$) which is always present in time-domain FLIM experiments. The gain of the polar approach over the fitting method is low but non negligible (<10%) for a limited range ($1.25 < \tau < 2.5$ ns when $T = 12.5$ ns). We emphasize the fact that this limited range coincides exactly with experimental lifetime values of fluorophores commonly used in FRET experiments (eGFP or CFP).

Note that, in this present work, we have supposed both theoretically and experimentally that the IRF of our FLIM acquisition system was a Dirac delta function. This assumption

which is valid for our specific system since the full width half maximum of its measured IRF is 32 ps (9) is not generally correct. In this case, in order to obtain exact lifetime values, it is necessary to deconvolute all fluorescence intensity decays from the experimental IRF before determining fluorescence lifetime with the polar approach or the fitting method. If this IRF deconvolution is correctly performed, the intensity decays become equivalent to those obtained with Dirac delta function. Consequently, all the results presented in this work are still valid.

For the simulated resolution and sensitivity studies provided here, we have considered particular lifetime values $\tau =$ 2.5 ns and fluorescence background N_b ($N_b = N/10$). While this is a usual lifetime value and a typical fluorescence background encountered in FLIM experiments (9), our study is also easily transposable to more general experimental conditions thanks to our theoretical F values treatment.

Finally, with our theoretical treatment presented here [Eq. (11)], when fluorescence background is present, we demonstrate that the least square method does not provide the best estimator of the lifetime parameter for fluorophores exhibiting mono-exponential intensity decays. In this study, we demonstrate indeed that the polar approach allows determining more accurate lifetime values for a limited range ($1.25 < \tau < 2.5$ ns when $T = 12.5$ ns and $b > 0.05$). This study could also be extended for samples emitting biexponential intensity decays (like in FRET experiments): $I(t) = a_1 \exp(-t/\tau_1) + (1 - a_1) \exp(-t/\tau_2)$. For such samples, it is possible to determine the lifetime components numerically by fixing the donor lifetime in the absence of acceptor τ_2 and by solving the system of Eqs. (6) and (7) (as described in Ref. 20). In this case, the polar approach continues to help, however with reduced benefits due to the necessity to fix one unknown parameter in order to determine other lifetime components. A theoretical treatment of these benefits in presence of background is under investigation.

Acknowledgments

The authors are grateful to Bernard Vandenbunder (IRI) for a critical reading of this manuscript. This work benefited from scientific discussions within the FLIM axis supported by RT-MFM, technological network of MRCT. The authors thank the imaging plateform BICFaL (Biophotonic and Imaging Core Facility of Lille).

Literature Cited

1. Lakowicsz JR. Principles of Fluorescence Spectroscopy. New York: Plenum Publishers; 1999.
2. Selvin PR. The renaissance of fluorescence resonance energy transfer. Nat Struct Biol 2000;7:730–734.
3. Jares-Erijman EA, Jovin TM. FRET imaging. Nat Biotechnol 2003;21:1387–1395.
4. Gadella TWJ, Jovin TM, Clegg RM. Fluorescence lifetime imaging microscopy (FLIM)—Spatial-resolution of microstructures on the nanosecond time-scale. Biophys Chem 1993;48:221–239.
5. Booth MJ, Wilson T. Low-cost, frequency-domain, fluorescence lifetime confocal microscopy. J Microsc (Oxford) 2004;214:36–42.
6. Leray A, Riquet FB, Richard E, Spriet C, Trinel D, Heliot L. Optimized protocol of a frequency domain fluorescence lifetime imaging microscope for FRET measurements. Microsc Res Tech 2009;72:371–379.
7. Becker W, Bergmann A, Hink MA, Konig K, Benndorf K, Biskup C. Fluorescence lifetime imaging by time-correlated single-photon counting. Microsc Res Tech 2004;63: 58–66.
8. Suhling K, French PM, Phillips D. Time-resolved fluorescence microscopy. Photochem Photobiol Sci 2005;4:13–22.
9. Waharte F, Spriet C, Heliot L. Setup and characterization of a multiphoton FLIM instrument for protein–protein interaction measurements in living cells. Cytometry A 2006;69A:299–306.
10. Spriet C, Trinel D, Riquet F, Vandenbunder B, Usson Y, Heliot L. Enhanced FRET contrast in lifetime imaging. Cytometry A 2008;73A:745–753.
11. Padilla-Parra S, Auduge N, Coppey-Moisan M, Tramier M. Quantitative FRET analysis by fast acquisition time domain FLIM at high spatial resolution in living cells. Biophys J 2008;95:2976–2988.
12. Digman MA, Caiolfa VR, Zamai M, Gratton E. The phasor approach to fluorescence lifetime imaging analysis. Biophys J 2008;94:L14–L16.
13. Jameson DM, Gratton E, Hall RD. The measurement and analysis of heterogeneous emissions by multifrequency phase and modulation fluorometry. Appl Spectrosc Rev 1984;20:55–106.
14. Clayton AH, Hanley QS, Verveer PJ. Graphical representation and multicomponent analysis of single-frequency fluorescence lifetime imaging microscopy data. J Microsc 2004;213 (Part 1):1–5.
15. Redford GI, Clegg RM. Polar plot representation for frequency-domain analysis of fluorescence lifetimes. J Fluoresc 2005;15:805–815.
16. Gerritsen HC, Asselbergs MA, Agronskaia AV, Van Sark WG. Fluorescence lifetime imaging in scanning microscopes: Acquisition speed, photon economy and lifetime resolution. J Microsc 2002;206 (Part 3):218–224.
17. Li DU, Bonnist E, Renshaw D, Henderson R. On-chip, time-correlated, fluorescence lifetime extraction algorithms and error analysis. J Opt Soc Am A Opt Image Sci Vis 2008;25:1190–1198.
18. Hall P, Sellinger B. Better estimates of exponential decay parameters. J Phys Chem 1981;85:2941–2946.
19. Köllner M, Wolfrum J. How many photons are necessary for fluorescence-lifetime measurements? Chem Phys Lett 1992;200:199–204.
20. Leray A, Spriet C, Trinel D, Heliot L. Three-dimensional polar representation for multispectral fluorescence lifetime imaging microscopy. Cytometry A 2009;75A: 1007–1014.
21. Philip J, Carlsson K. Theoretical investigation of the signal-to-noise ratio in fluorescence lifetime imaging. J Opt Soc Am A 2003;20:368–379.
22. Zhong H, Wu X, Huang H, Fan Q, Zhu Z, Lin S. Vertebrate MAX-1 is required for vascular patterning in zebrafish. Proc Natl Acad Sci USA 2006;103:16800–16805.
23. Barber PR, Ameer-Beg SM, Gilbey J, Carlin LM, Keppler M, Ng TC, Vojnovic B. Multiphoton time-domain fluorescence lifetime imaging microscopy: Practical application to protein–protein interactions using global analysis. J R Soc Interface 2009;6:S93–S105.